Forest Ecology and Management 262 (2011) 1950–1962

Contents lists available at SciVerse ScienceDirect

Forest Ecology and Management

journal homepage: www.elsevier.com/locate/foreco

Tree size distribution at increasing spatial scales converges to the rotated sigmoid curve in two old-growth beech stands of the Italian Apennines

Alfredo Alessandrini [a], Franco Biondi [b], Alfredo Di Filippo [a], Emanuele Ziaco [a], Gianluca Piovesan [a,*]

[a] DendrologyLab, Department of Agriculture, Forests, Nature and Environment (DAFNE), Università degli Studi della Tuscia, Via S.C. de Lellis, I-01100 Viterbo, Italy
[b] DendroLab, Department of Geography, MS 154, University of Nevada, Reno, NV 89557, USA

ARTICLE INFO

Article history:
Received 5 May 2011
Received in revised form 9 August 2011
Accepted 14 August 2011
Available online 28 September 2011

Keywords:
Old-growth
Beech
Forest structure
Community dynamics
Deadwood
Shifting mosaic

ABSTRACT

Tree size distributions of old-growth forests are a fundamental tool for both scientific analysis and conservation management. In old-growth forests the diameter distribution shape may depend on spatial scale, but theoretical models often show fundamental similarities that suggest general underlying mechanisms controlling regeneration, mortality, and growth under different disturbance regimes. In this study we investigated the horizontal structure of two old-growth beech (*Fagus sylvatica* L.) forests in central Italy using a series of spatial scales and analytical approaches. Individual plots (each one 0.13 ha in size) were progressively aggregated into larger groups to simulate an increase in sampled area. A third-order polynomial was fit to the diameter distributions of the aggregated areas, and the curves were ranked by the AIC method. The rotated sigmoid (RS) shape was the most common descriptor of tree size distributions, and became dominant once aggregated spatial scales exceeded 0.6–0.8 ha. The same result was obtained when a single plot was made progressively larger. Given the relatively small scale (starting from 0.1 ha) at which the RS model emerged, old-growth beech forests of the Italian Apennines show a complex, yet highly resilient structure, recognizable even in small (<1 ha) patches. Most likely, the rotated sigmoid structure is a function of endogenous structural processes (e.g. self-thinning) in this shade-tolerant species in combination with intermediate-to-fine-scale disturbance (which especially impacts the largest trees) and resulting gap dynamics.

1. Introduction

Diameter size distributions of uneven-aged forests have been extensively studied as a tool for quantifying structural development (Goff and West, 1975; Zenner, 2005) and evaluating disturbance impacts (Baker et al., 2005; Coomes and Allen, 2007), but there is no consensus in the literature regarding what distribution shapes are most common in old-growth stands. A commonly adopted model for the diameter (i.e. horizontal) structure of tree populations is the reverse-J distribution (e.g. Rubin et al., 2006), but recent analytical and theoretical developments have expanded the range of models that appear appropriate for uneven-aged stands (Wang et al., 2009). In particular, hyperbolic functions have been derived from the Metabolic Theory of Ecology (MTE), which considers the relationships between organism size, temperature, and metabolic rates as the controlling factors behind most observed ecological patterns (Brown et al., 2004). This theory has found little empirical support in forest populations (e.g. Wang et al., 2009), possibly because disturbance processes play a greater role in shaping old-growth forest structures (Enquist et al., 2009). In fact, studies based on demographic processes have shown that mortality rates are not constant, rather they tend to be U-shaped, as they are greater at both ends of the diameter distribution than in its middle portion (Lines et al., 2010).

A commonly observed model for stem size distribution in old-growth forest populations is the rotated sigmoid curve (Goff and West, 1975; Gove et al., 2008). From an ecological point of view, this size distribution model is closely linked to U-shaped mortality processes (Lorimer et al., 2001; Leak, 2002) and is commonly found in forest ecosystems where stand dynamics are controlled by competition for light. A recent study of old-growth beech forests has indeed pointed out that rotated sigmoid curves well represent their size distributions (Westphal et al., 2006). While some authors have argued that this theoretical shape arises because of undersampling, i.e. when sampled plots are too small (e.g. Rubin et al., 2006), other studies have used progressively larger sampling areas to show how the rotated sigmoid often becomes the dominant model as spatial scales increase (e.g. Janowiak et al., 2008).

Because the type and number of development stages and phases in a forest cycle may depend on specific bioclimatic environment and disturbance processes (e.g. Král et al., 2010), and on the tolerances and ecophysiological requirements of forest species, it

* Corresponding author. Tel.: +39 0761 357387, mobile: +39 380 4399787; fax: +39 0761 357250.
E-mail address: piovesan@unitus.it (G. Piovesan).
URL: http://www.daf.unitus.it/dendro/ (G. Piovesan).

0378-1127/$ - see front matter © 2011 Elsevier B.V. All rights reserved.
doi:10.1016/j.foreco.2011.08.025

is paramount to expand investigations on tree size distributions to include as many forest ecosystems as possible. At the same time, it is essential to establish an objective methodology to determine the minimum sampling area needed to obtain a convincing representation of the horizontal structure of a stand. An effective method for removing model dependence on spatial scales consists of progressively aggregating sample plots and then to determine the best curve fit for stem size distribution on such increasing areas (Janowiak et al., 2008). During this process, it is possible to develop hypotheses on the mechanisms that generate a stable diameter distribution. The combined area at which the model fit no longer changes can also be used to determine a minimum sampling requirement for the forest type under study. A similar approach has been adopted in ecology for analyzing and quantifying plant biodiversity using the species accumulation curve (Gotelli and Colwell, 2001).

An uneven-aged silvicultural system adopted in Alpine forests, the "plenter" system (O'Hara and Gersonde, 2004), has been successful at producing large trees for over a century. This empirically-based management practice has generated beech (and spruce) populations whose size distribution is closely represented by a rotated sigmoid curve (Schütz, 2006). In order to infer mechanisms that underlie the generation of this model in temperate forest ecosystems (Gove et al., 2008), one could then compare the structure of these highly managed forests with old-growth beech stands having much greater degree of naturalness (Sagheb-Talebi and Schütz, 2002). Old-growth beech forests in the Italian Apennines are an ideal case study for investigating how tree distributions can be represented by various theoretical models. Several of these high-elevation *Fagus sylvatica* stands are dominated by the oldest (400–550 years) beech trees in Europe (Piovesan et al., 2005b, 2010) under a variety of ecological conditions (elevation, topography, fertility) and a low-severity disturbance regime (Piovesan et al., 2011).

In this paper we analyzed the horizontal structure of two beech forests showing different old-growth conditions, with the objective of determining which model, and which spatial scale, best represents their tree size distribution. Since diameter distribution models for uneven-aged forests, either managed or old-growth, have been developed using either a few large plots (full calliperings of coherent areas >1 ha and up to 10 ha; e.g. Westphal et al., 2006), or many small plots (~0.1 ha or smaller, down to 0.04 ha e.g. Schwartz et al., 2005; Coomes and Allen, 2007; D'Amato et al., 2008; Gove et al., 2008; Gronewold et al., 2010), results obtained from aggregating small circular plots scattered throughout the forest were tested by progressively increasing the size of a continuous plot (concentric circular areas). Finally, a comparison was performed against published data for "plenter" managed forests, in order to define a suitable target model and guide conservation strategies that enhance resilience and sustainability of old-growth beech forest ecosystems.

2. Materials and methods

Our study areas, Valle Cervara (VCH) and Coppo del Principe (COP), are located in the central Italian Apennines, within the NW corner of the Abruzzo-Lazio-Molise National Park (PNALM; Abruzzi region, L'Aquila province). VCH lies in the town district of Villavallelonga, COP in that of Pescasseroli. Both forests cover slopes from 1500–1600 m to the treeline (1800–1900 m asl), but VCH has a prevailing N–NW aspect and COP a prevailing NE aspect (Table 1). Bedrock consists of Cretaceous limestone; soils can be referred to the brown group (Piovesan et al., 2005b). Climate regime at both sites can be described as Mediterranean montane, with cold snowy winters and dry summers (Piovesan et al., 2005b). Orographic precipitation at these high-elevations sites (annual precipitation at VCH is about 1500 mm/year; Piovesan et al., 2008) provides favorable conditions for the establishment of a mesic hardwood deciduous forest (*Polysticho-Fagetum*; Feoli and Lagonegro, 1982).

Sampled stands occupy the upper beech altitudinal range in central Italy so they can be ascribed to the bioclimatic zone of high-elevation beech forests, whose growth is mainly limited by spring temperature (Piovesan et al., 2005a). Prior to becoming a national park, the two forests escaped logging because of difficult access and their protective function against avalanches and landslides (Piovesan et al., 2005b). VCH can be considered a primary multi-cohort forest (Frelich, 2002), with no signs of past human exploitation (Piovesan et al., 2005b). The COP stand also showed no signs of logging, several senescent and dying individuals, and a heterogeneous vertical/horizontal structure. Multi-century trees are present, reaching 340–400 years at COP and exceeding 500 years at VCH, where we identified the oldest known *Fagus* tree in the Northern Hemisphere (Piovesan et al., 2005b). From a structural point of view, the two study forests are uneven-aged, with old-growth indicators above the thresholds commonly reported for mesic hardwood deciduous forests (Table 2; also see Piovesan et al., 2005b, 2010). In particular, both stands were characterized by high values of tree basal area and volume, with many large individuals, which typically account for most volume in old-growth forests. The deadwood component was similarly abundant (11–13% of living volume), including several large (diameter at breast height, dbh > 67.5 cm) snags per hectare.

Field sampling was initially based on circular plots with a 20-m radius, scattered within areas with minimal human impact. The 18 plots sampled at Valle Cervara in 2003 (Piovesan et al., 2005b) were considered at first, then we focused on a primary old-growth area (Figs. 1 and 9) that harbors the oldest European beech trees yet reported (Piovesan et al., 2011), including a recently identified 560-year old individual. Inside this core stand, which is split by an old avalanche tract (see Fig. 9), 11 scattered plots had been sampled in 2003, and nine more were sampled in 2010. In each plot, all living trees with dbh > 2.5 cm were measured; deadwood was also sampled as reported in Piovesan et al. (2010). Snags were quantified by size class as percentage of the live tree density for that size class. Diameter distributions were developed using 5 cm diameter classes starting from 2.5 cm. When no trees of a certain dbh class were present inside a plot, such absence was recorded either as zero (the coding used by Janowiak et al., 2008) or as a missing observation, which may be more appropriate given the

Table 1
Summary of geographical features for the two study areas.

Site	Code	Latitude (°N)	Longitude (°E)	Elevation (m asl)	Slope (%)	Main aspect	Stand area (ha)	Sampled area (ha)	Plots *N* (Year)
Valle Cervara	VCH	41.828	13.732	1700–1850	40–60	N–NW	24	2.26	18[a] (2003)
								1.38	11[b] (2003)
								1.13	9[b] (2010)
								0.75	6[c] (2011)
Coppo del Principe	COP	41.788	13.738	1500–1750	20–60	NE	45	0.88	7[a] (2009)

[a] Scattered plots (all stand).
[b] Scattered plots (old-growth core area).
[c] Contiguous concentric plots (old-growth core area).

Table 2
Summary of structural features for the two study areas.

Site (Year)	Live trees structure								Dead trees structure		Age structure	
	Stem ha^{-1}						m^2 ha^{-1}	m^3 ha^{-1}	m^3 ha^{-1}	Stem ha^{-1}	Years	Years
	N	VST	ST	MT	LT	VLT	BA	V	DW	Snags	Age_{max}	Age_5
Valle Cervara (2010)	818	620	35	49	72	42	38	545	59	27	560	507
Coppo del Principe (2009)	296	108	14	46	52	76	44	715	91	28	378	344

N = stand density (trees with diameter at breast height (dbh) $\geqslant$ 2.5 cm); VST = density of very small trees (2.5 cm $\leqslant$ dbh < 17.5 cm); ST = density of small trees (17.5 cm $\leqslant$ dbh < 27.5 cm); MT = density of medium trees (27.5 cm $\leqslant$ dbh < 42.5 cm); LT = density of large trees (42.5 cm $\leqslant$ dbh < 57.5 cm); VLT = density of very large trees (dbh $\geqslant$ 57.5 cm); BA = basal area; V = woody volume of living trees; DW = deadwood volume; Snags = density of snags (dbh $\geqslant$ 10 cm); Age_{max} = age of the oldest tree cored in the stand; Age_5 = mean age of the five oldest trees cored in the stand.

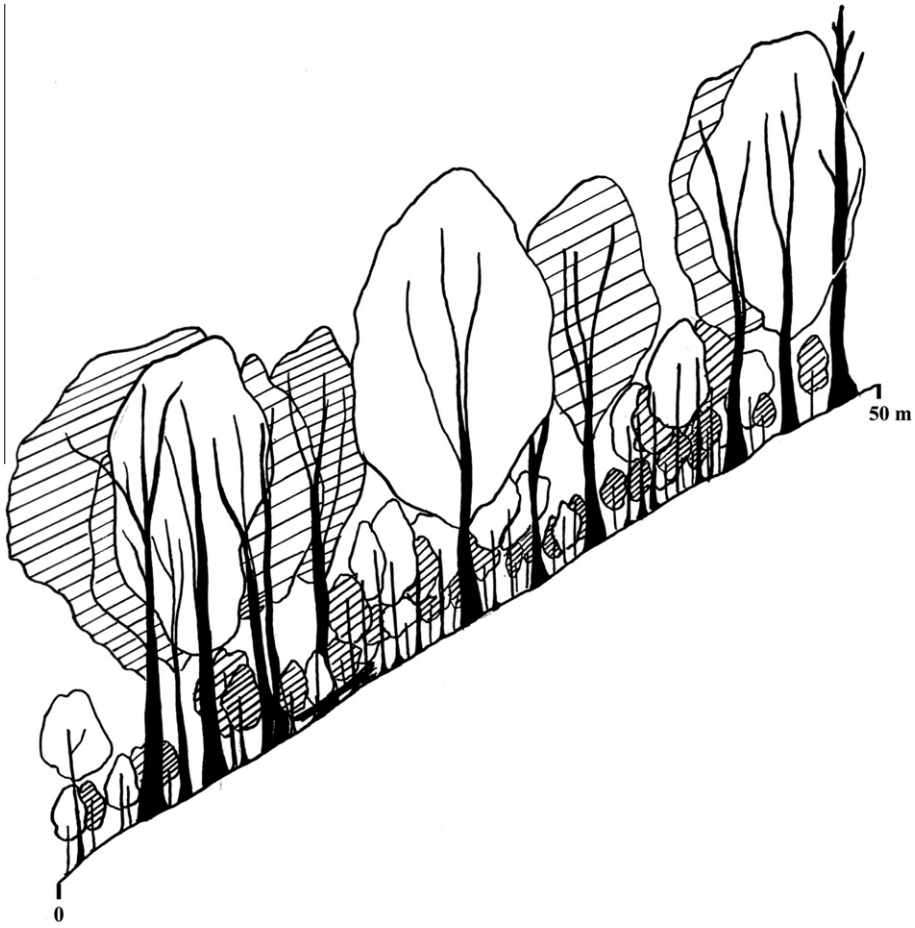

Fig. 1. Vertical structure of the Valle Cervara old-growth beech forest, recorded along a 20 × 50 m transect. All trees shown in the sketch are *Fagus sylvatica* L.; shaded crowns represent trees in the background.

relatively small size (0.13 ha) of each plot (see Noel et al., 1998). When the absence of a certain dbh class was recorded as zero and because the logarithm of zero is undefined, 1.0 was added to all values of trees per hectare (tph) before transformation (Janowiak et al., 2008).

In order to simulate how diameter distributions changed as the sampling area increased, individual scattered plots were aggregated by means of *k*-combination without repetitions; hence subsets comprised of distinct *k* elements of the total number of plots (*n*) ranged from 1 to *n*. This was done separately by site and year, so that, for example, the nine plots available for Valle Cervara in 2010 simulated spatial scales up to 1.13 ha at 0.13 (0.1256) ha intervals. Diameter distributions were also studied by progressively increasing the area of a sampling plot by means of concentric circular areas, starting at 0.13 ha and expanded by 0.13 (0.1256) ha increments up to 0.75 ha. This method minimized boundary effects while allowing the analysis of changing spatial scales in comparison with the aggregation method. The starting 0.13-ha plot had an initial diameter distribution that was far from the rotated sigmoid one (see Fig. 7).

A logarithmic scale was used for density, as normally done for uneven-aged populations, and polynomials up to the third-order were fit to the diameter distribution of each aggregated or concentric sample area using ordinary least squares (e.g. Janowiak et al., 2008). The best significant ($P < 0.05$) model among all possible combinations was selected using the AIC criterion (Akaike, 1974). Adjusted R^2 and root mean square error (RMSE) were then computed for the selected model. The diameter distribution shape was named according to the terminology used in Table 2 of Janowiak et al. (2008). An additional model we encountered, defined

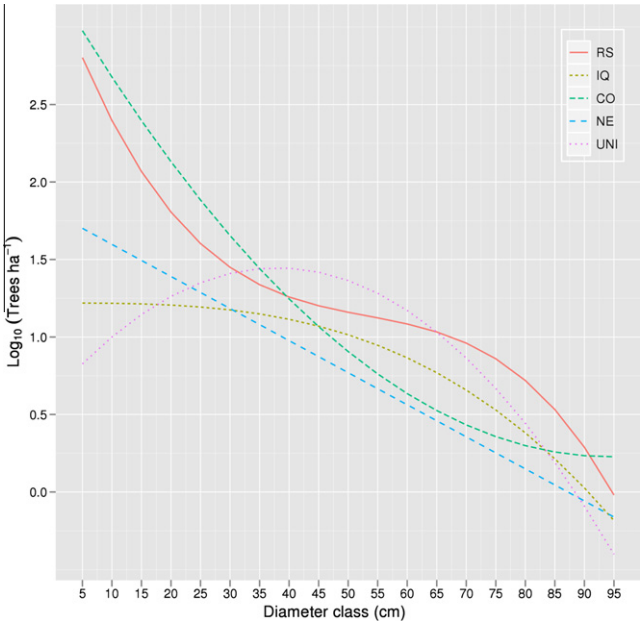

Fig. 2. Diameter distribution shapes present in old-growth beech forests of the Italian Apennines. The shapes were selected using signs of significant ($P < 0.05$) coefficients in a third-order polynomial fit to the diameter distribution (Janowiak et al., 2008). IQ = increasing-*q*, NE = negative exponential, UNI = unimodal, CO = concave, RS = rotated sigmoid.

by a negative coefficient for dbh and dbh^2, plus a non-significant coefficient for dbh^3, was assigned to the increasing-*q* category. Spatial dependence of forest structure (i.e. selected model in each plot) was analyzed using two-dimensional sample variograms and isotropic models (Isaaks and Srivastava, 1989) for 40-m distance intervals up to a 240-m maximum.

A space-for-time approach was employed to investigate structural changes over time (Watt, 1947) using abundance of different size classes as an indicator of the developmental stage of a forest, or, in other words, of the phase reached by the tree population in the structural cycle (e.g. Král et al., 2010). As commonly done when assessing uneven-aged forest management practices (e.g. Sagheb-Talebi and Schütz, 2002), we subdivided the range of measured dbh values in a few categories using traditionally accepted intervals for Italian silviculture (Piovesan and Portoghesi, 1993). Our five categories were very small trees (VST, dbh classes 5–15 cm), small trees (ST, dbh classes 20–25 cm), medium trees (MT, dbh classes 30–40 cm), large trees (LT, dbh classes 45–55), and very large trees (VLT, dbh classes $\geqslant$60 cm), and their abundance was quantified in each sampled plot. We then performed a principal component analysis (PCA, Jolliffe, 1986) based on the correlation matrix of these abundance values, plus the deadwood volume, at all sampled plots, including both sites and both years. Most numerical computing was done in the R software environment (R Development Core Team, 2010).

3. Results

Tree size distributions (Fig. 2) were well described by the five models identified by Janowiak et al. (2008). Diameter distribution convergence to the rotated sigmoid shape at spatial scales >0.8 ha was observed in 95% or more of all possible combinations of the 18 original scattered plots sampled at Valle Cervara in 2003 (Fig. 3 and Fig. S1). While aggregated sampled area had a clear influence on the shape of the model fit to the tree size distribution at very small scales (Fig. 4), it became unimportant for spatial scales larger than about 0.6 ha. This result was robust with respect to the area under study (either old-growth forest or primary core area of old-growth forest) and year of sampling, as well as coding convention used to report dbh size classes with no tallies (Fig. 5). As the combined surface of sampled plots increased, distribution shape converged to the rotated sigmoid at both Valle Cervara (Figs. 5 and 6, Figs. S2 and S3) and Coppo del Principe (Figs. S4–S6) beech forests, and for both 2003 and 2010 years at the same study site (Valle

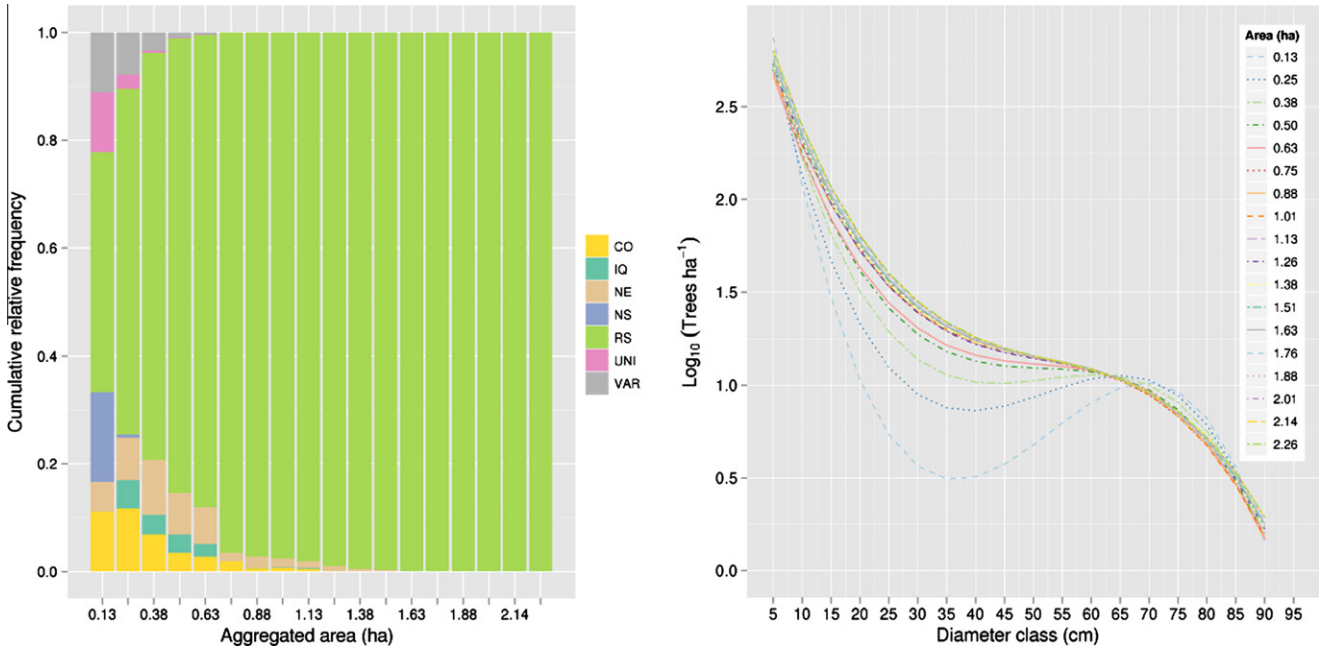

Fig. 3. Effect of increasing spatial scales, obtained by aggregating more and more circular plots (18 total, each one 0.13 ha in size, sampled in 2003 at Valle Cervara) scattered throughout the forest. Absence of a dbh class in a plot was coded as zero. For goodness-of-fit statistics see Fig. 4. (Left) Cumulative relative frequency of diameter distribution shapes (see Fig. 2 for the codes of the five main models; NS = non-significant model ($P > 0.05$); VAR = variable). (Right) Evolution of the rotated sigmoid diameter distribution with increasing sampled area. At each spatial scale the curve is the average of the significant rotated sigmoid distributions (green bars in the figure on the left). The rotated sigmoid converges to a final model at aggregated areas of about 0.6 ha. (For interpretation of the references to color in this figure legend, the reader is referred to the web version of this article.)

Cervara). Model goodness-of-fit indicators (adjusted R^2 and RMSE) showed that combinations of five or more plots were enough to capture the rotated sigmoid distribution (Fig. 4, Figs. S2, S3 and S6). For progressively larger concentric areas, the rotated sigmoid distribution became the model of choice at spatial scales larger than 0.5 ha (Fig. 7 and Fig. S7). Based on the spatial evolution of the sigmoidal shape and on the goodness-of-fit results (Fig. 7), the RS model for the 0.75-ha area is not only stable but also closely resembles the shape obtained by aggregating plots scattered over the whole population (Fig. 8).

Convergence to the rotated sigmoid shape occurred for slightly smaller aggregated areas when a dbh class with no tallies was considered a missing observation (see Fig. S1 for all Valle Cervara plots sampled in 2003). More variable (“noisier”) distribution models were selected for small aggregated areas (<1 ha) when absence of a dbh class in a sampled plot was coded as zero. In particular, “reverse J-type” shapes (such as the negative exponential) and the increasing-q shape appeared more often under this coding scheme (Figs. 3 and 5 vs. Fig. S1). At Coppo del Principe (Fig. S4), unimodal distributions for small aggregated areas were selected more frequently than at Valle Cervara. At that site, when absence was coded as missing, distribution shape was non-significant in a few more cases than at Valle Cervara, mostly because the unimodal (UNI) and concave (CO) distribution were not recognized (see left vs. right panel of Fig. S4).

The final shape of the rotated sigmoid curve was not heavily affected by coding option, i.e. zero vs. missing, used to identify absence of a dbh class (Figs. 6 and 7, and Fig. S5). As soon as the aggregated sampled area exceeded 0.6 ha, the shape of the curve remained essentially stable using either method in both space and time. However, at Valle Cervara, and particularly for the 2003 field campaign, there was a large difference between the shape of the rotated sigmoid for the smallest areas (<0.3–0.4 ha) compared to larger ones. When zero values were used, the absence of small and medium-size dbh classes pushed further downward the initial decreasing portion of the rotated sigmoid curve (Fig. 6). Interestingly, the evolution of the rotated sigmoid curves as shown by the aggregation of multiple plots compensates for this coding difference. A direct comparison between average diameter distribution of individual plots that were modeled using a rotated sigmoid at Valle Cervara core area for the three different sampling years (Fig. 8), revealed a remarkable level of overlap, suggesting

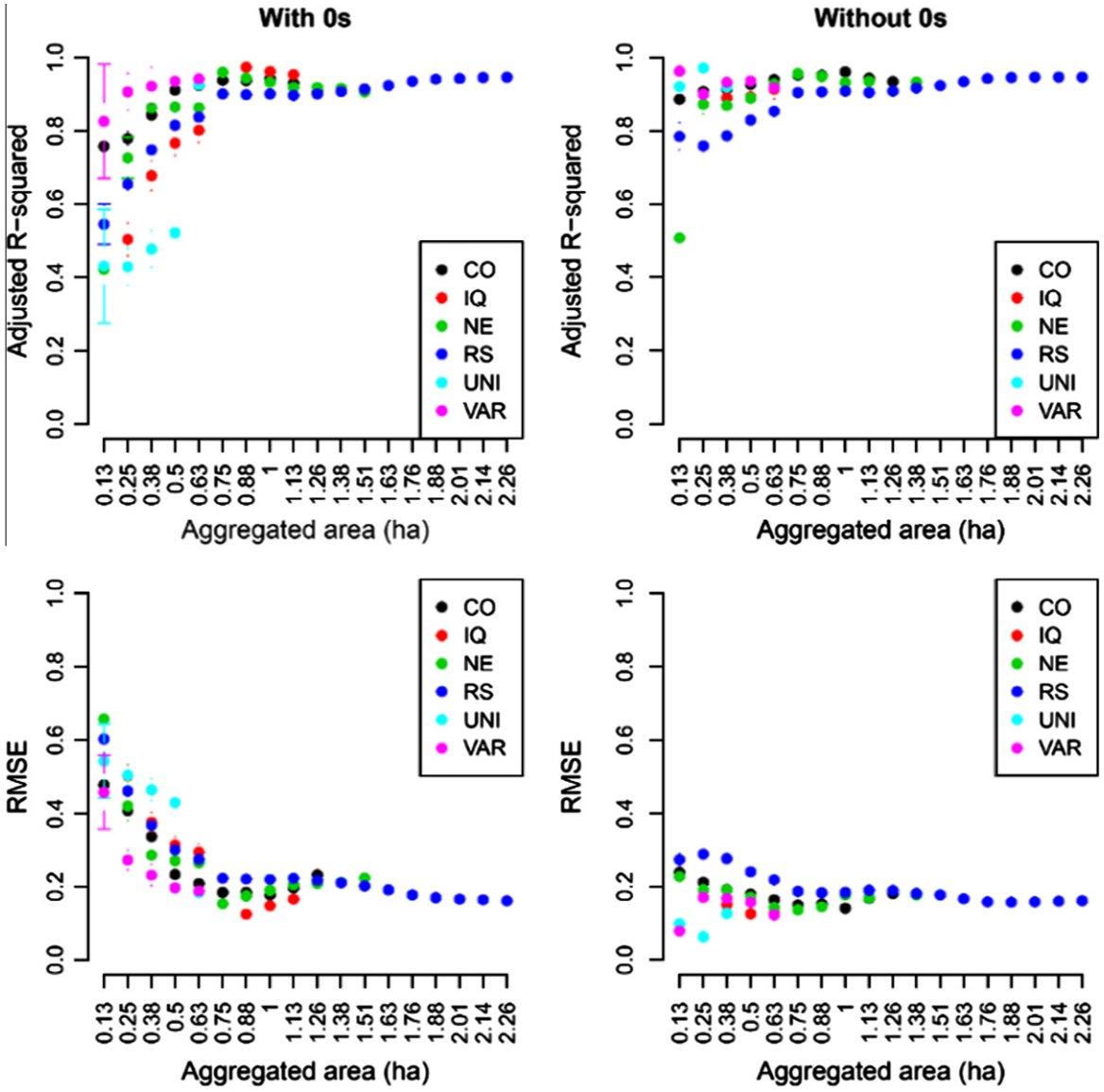

Fig. 4. Adjusted R^2 and RMSE value at increasing spatial scales, shown by aggregating more and more scattered sample plots (18 total, each one 0.13 ha) sampled in 2003 at Valle Cervara. The two methods to report absence of a dbh class in a plot are compared: (Left) absence coded as zero; (Right) absence coded as missing value.

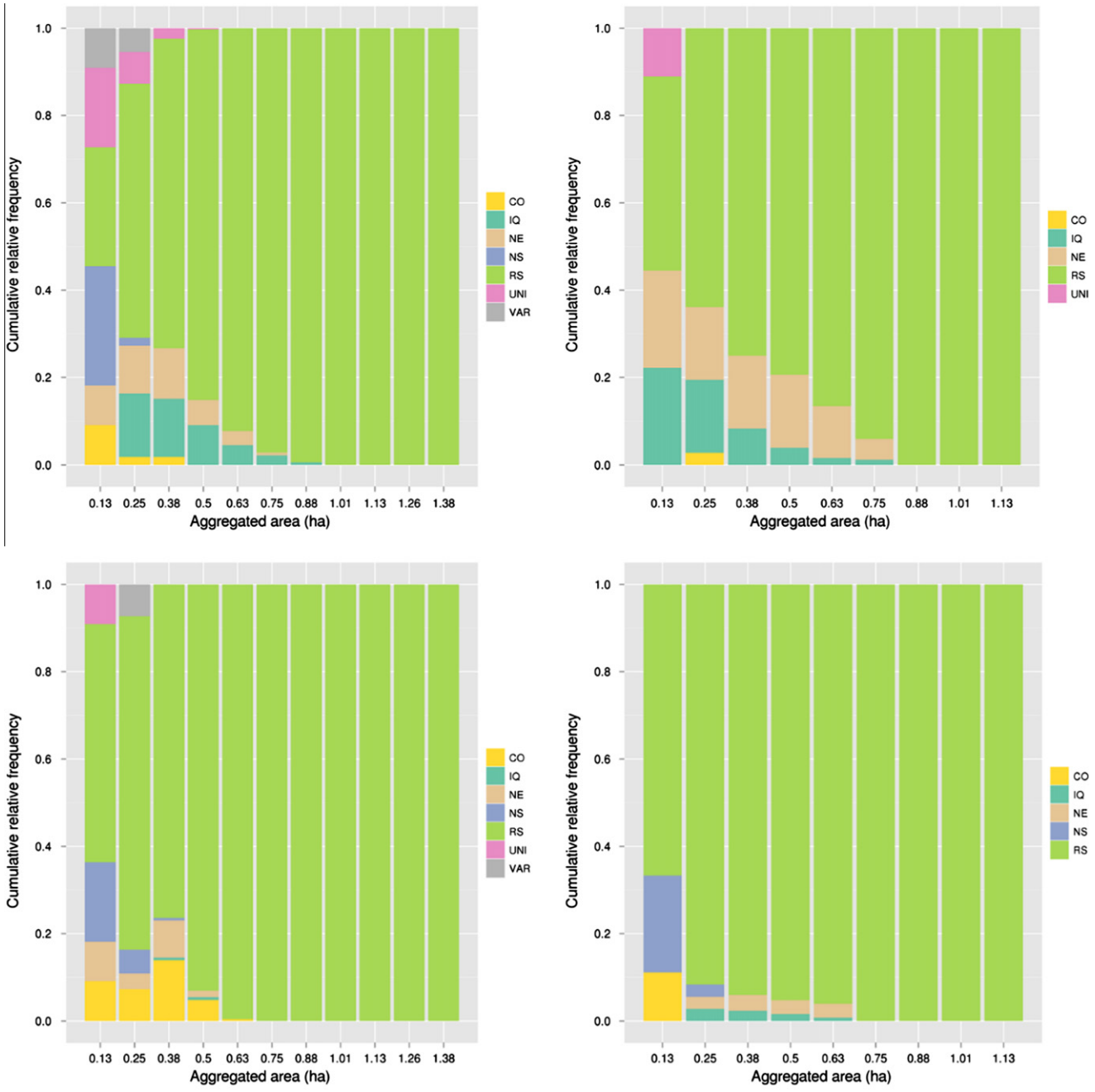

Fig. 5. Cumulative relative frequency of diameter distribution shapes for the Valle Cervara core area (primary old-growth stand) comparing two different years of sampling and two methods to report absence of a dbh class in a plot. For goodness-of-fit statistics see Figs. S2 and S3. (Left) Scattered plots (11) sampled in 2003; (Right) scattered plots (9) sampled in 2010. (Top) Absence coded as zero; (Bottom) absence coded as missing value.

temporal stability of the rotated sigmoid shape even at small scales. Size distribution models were spatially autocorrelated (Fig. 9 bottom), with a tendency for the dominant shape (mostly the RS) to remain unchanged over distances up to about 60 m. These spatial relationships between forest structures remained stable from 2003 to 2010, especially when absence of a dbh class was coded as missing value (Fig. 9 top).

The first two principal components of dbh categories (VST, ST, MT, LT, VLT) in all plots, together with deadwood, explained more than half of the variance (35.3% PC1, and 22.0% PC2). The PCA plot of selected distribution shapes, superimposed with a biplot of the original dbh categories and deadwood (Fig. 10), revealed a strong connection between tree size distribution and development phase in the structural cycle of a forest. The graph uncovered an inverse relationships between areas dominated by medium (MT) to large (LT) trees as opposed to areas where very small (VST) trees are more abundant. In fact, the biplot axis for VST is almost exactly opposite to that for LT. Basal area was most correlated ($r = 0.51$, $P = 0.006$) with the second principal component, since total basal area is usually greater where large trees dominate, a typical feature of old-growth forests (Sagheb-Talebi and Schütz, 2002). The order of the biplot axes highlights the structural cycle of old-growth forests, as it progresses counterclockwise from the lowest (VST) to the largest (VLT) dbh categories. Deadwood biomass (DW) falls close to the LT and VLT area, as larger individuals typically contribute the most to this component of forest biomass (Marage and Lemperiere, 2005).

Overall, by arranging individual plots in principal component space (Fig. 10), we were able to capture most temporal phases of

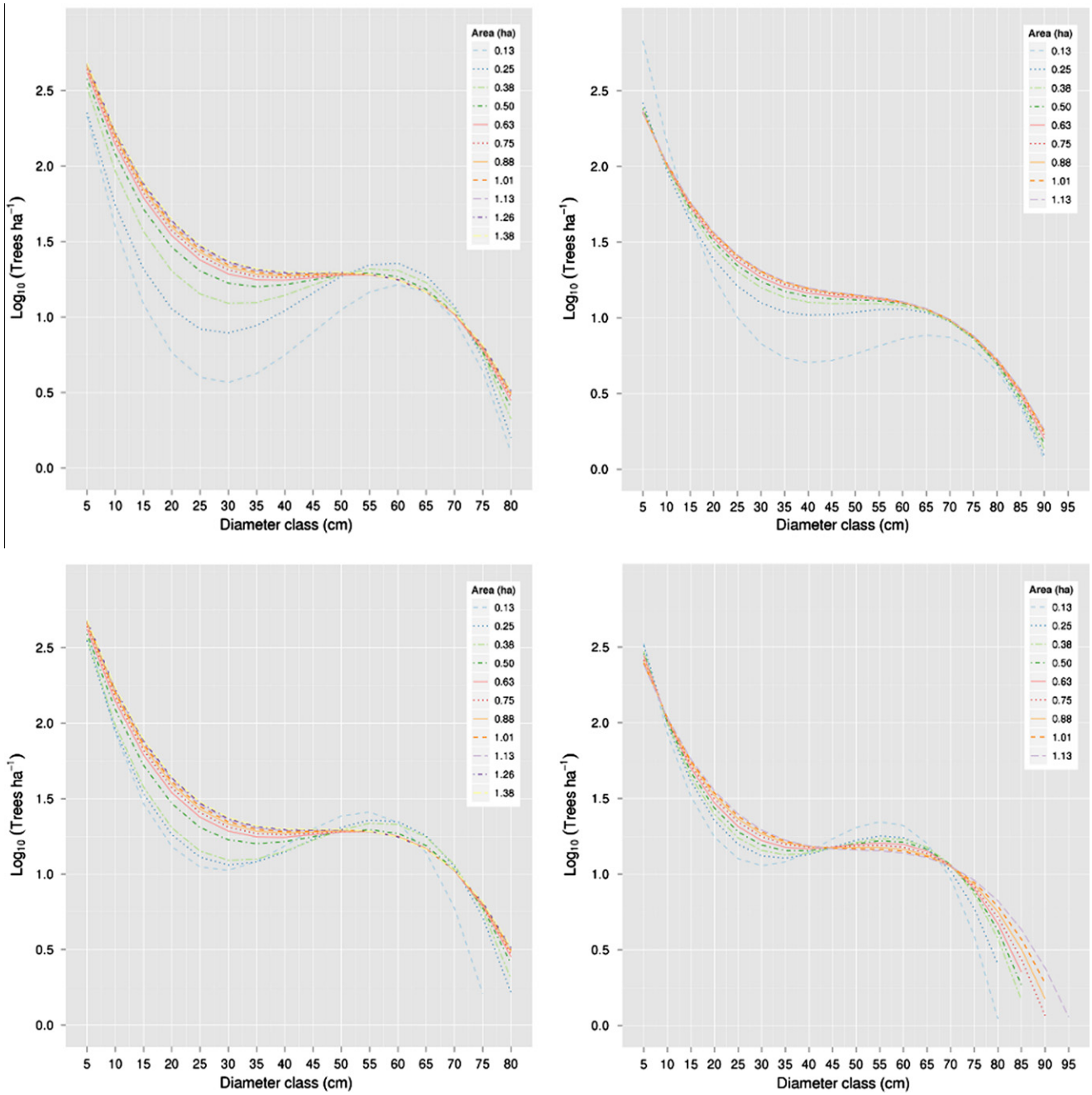

Fig. 6. Evolution of the rotated sigmoid diameter distribution shape at Valle Cervara core area (primary old-growth stand) with increasing sampled area, obtained by aggregating more and more scattered sample plots. At each spatial scale the curve is the average of the significant rotated sigmoid distributions. For goodness-of-fit see Figs. S2 and S3. The rotated sigmoid converges to a final model at aggregated areas of about 0.6 ha regardless of sampling year or method used to report absence of a dbh class in a plot. (Left) Plots (11) sampled in 2003; (Right) plots (9) sampled in 2010. (Top) Absence coded as zero; (Bottom) absence coded as missing value.

the structural cycle: aggradation, biostasis, and degradation (Oldemann, 1990; Peters, 1997). The innovation phase was not included in the analysis (and only mentioned in parenthesis within the graph) because no data on tree regeneration were considered in the PCA. Size distribution models tend to follow the structural phases even at very fine scales, given that each plot is 0.13 ha. The rotated sigmoid curve is absent in plots occupied by medium to large trees, while it becomes the model of choice in the center of the principal component graph, and when very small trees (VST) are most abundant. This suggests that a developed old-growth structure can be recognized even on extremely small areas, as long as they are not dominated by intermediate to large size classes. In fact, the late aggradation and biostasis phases are characterized by the greatest total basal area, and by a mostly unimodal size distribution when absence was coded as zero (Fig. S8). Notably, several non-significant size distribution models are located close to the deadwood axis, suggesting that the forest population, during the degradation phase of the structural cycle, can produce both a large amount of dead material and an irregular tree size distribution.

The stand-level rotated sigmoid curves obtained over time and over space provide information on the ecological development of beech forest populations (Fig. 11). It is clear that Valle Cervara has a well-developed, stable, and widespread old-growth structure, as the rotated sigmoid curves obtained by sampling different plots in 2003 and 2010 are remarkably similar. Our previous

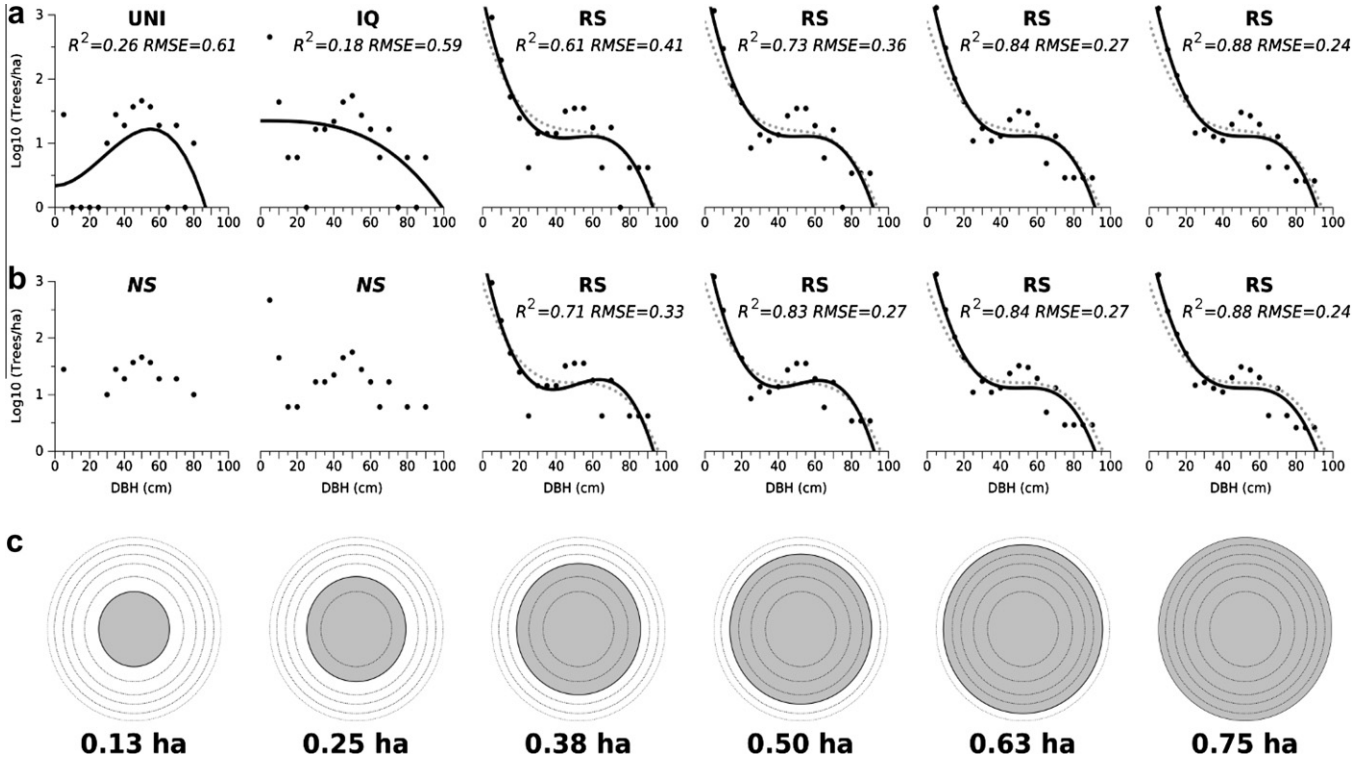

Fig. 7. Concentric circular plots sampling method at Valle Cervara old-growth core area. Effect of increasing spatial scales is shown by expanding concentric sample plots (each one 0.13 ha). The modeled mean diameter distribution of the 2010 scattered sample plots (gray dotted line) is also shown. (a) Absence coded as zero (R^2 = adjusted R^2); (b) absence coded as missing value; (c) area of the circular plot.

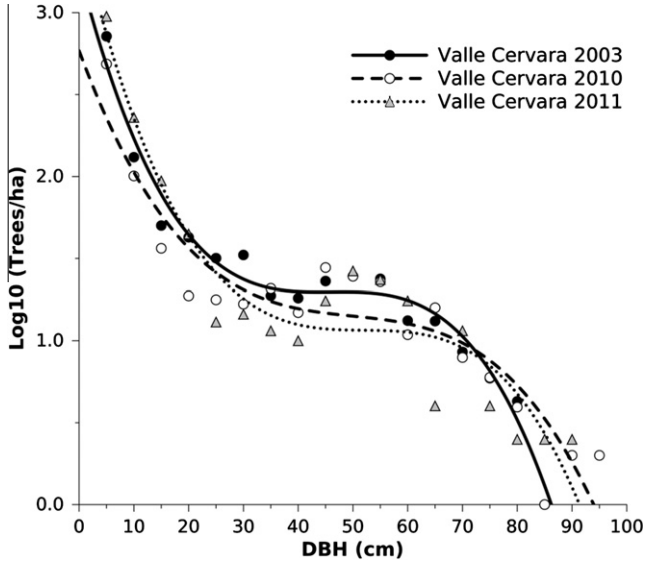

Fig. 8. Average diameter distribution modeled using a third-order polynomial – rotated sigmoid – at Valle Cervara old-growth core area for the two sampling methods in three different years: scattered (year 2003, 11 plots, total sampled area 1.38 ha; year 2010, 9 plots, total sampled area 1.13 ha) and concentric plots (year 2011, total continuous sampled area 0.75 ha).

studies (e.g. Piovesan et al., 2005b, 2011) had already shown that this forest was a prime example of *Fagus* old-growth stands, also containing the oldest (>500 years) beech trees in Europe. A reduction over time in the presence of trees with 20–30 cm dbh was likely due to an increase in mortality among the smallest sizes (as shown later – see Fig. 12), causing slower outgrowth into the medium dbh classes and/or a release of the surviving trees that would then quickly grow through this size category. Coppo del Principe and Valle Cervara RS distributions showed a mild divergence for these 20–30 cm stem sizes, but were otherwise in closer agreement for all other dbh classes. The similarity of distribution shape for large dbh classes indicates a convergence between these two forest populations with respect to structural processes that determine the presence of the oldest and largest trees. Comparing our stand-level rotated sigmoid curves with that of the plenter system (Schütz, 2006) revealed an expected difference for large sizes (Fig. 11), since logging preferentially targets the bigger trees. On the other hand, the overall shape of the plenter rotated sigmoid was parallel to ours, and almost overlapped the Valle Cervara curves for dbh less than 40 cm.

4. Discussion

By evaluating tree size distribution models for increasing spatial scales, as proposed by Janowiak et al. (2008), it was possible to systematically determine the genesis of the most representative shape for old-growth beech stands. In order to adequately capture the structure of a forest, sampling plots are supposed to be scattered as much as possible over the landscape (Rubin et al., 2006); for both fixed-area and prism sampling, Grenier et al. (1991) found that more dispersed sampling locations provide greater probability of obtaining a sample diameter distribution not significantly different from the underlying population distribution. Therefore, the aggregation of scattered circular plots was appropriate for understanding the minimum area and the type of numerical processing that are required to capture stand structure. Following this approach, stable uneven-aged patterns in old-growth beech forests of the Italian Apennines were recognized even at aggregated spatial scales of 0.6–0.8 ha. While distribution models for smaller areas included the rotated sigmoid, negative exponential, and

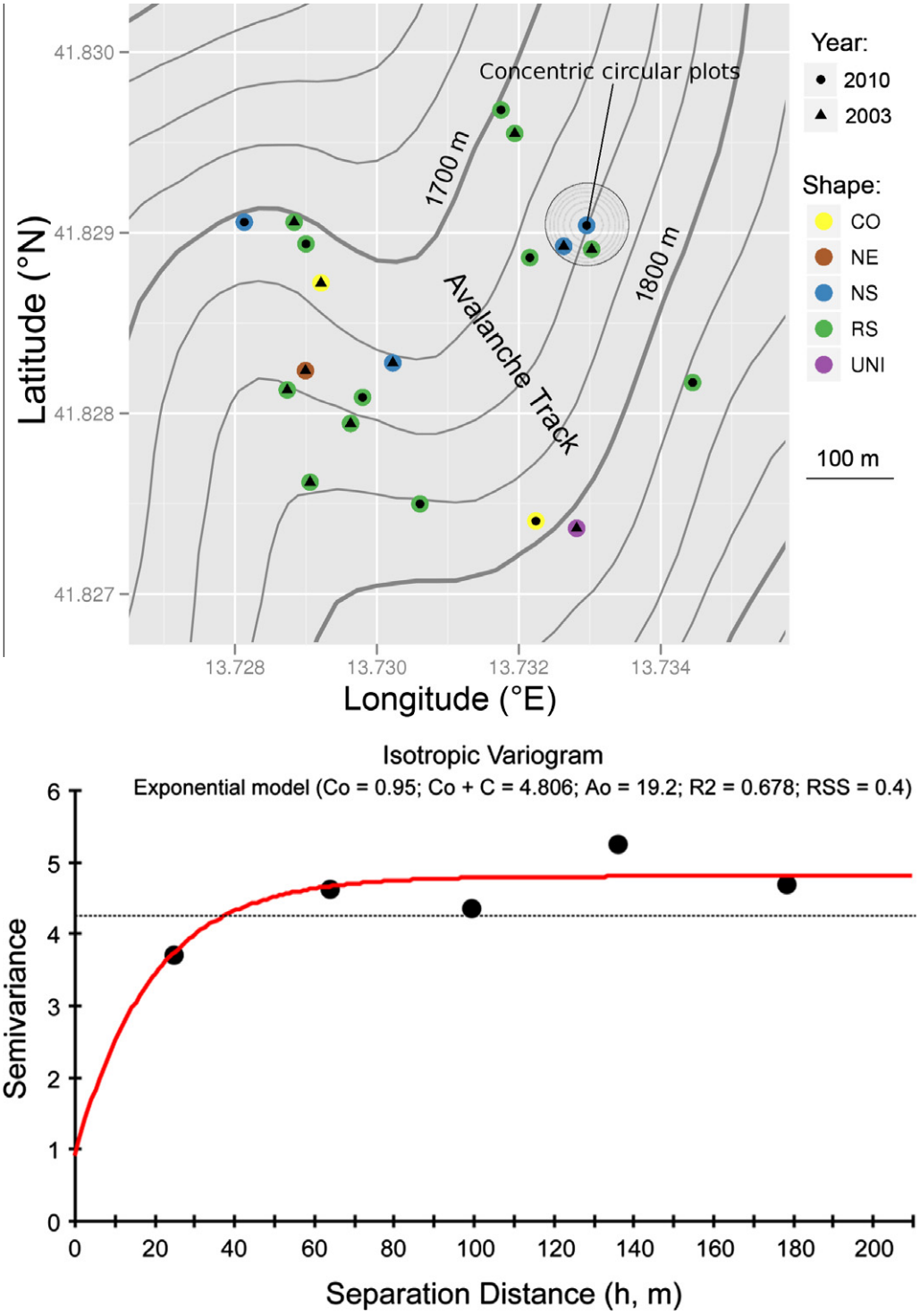

Fig. 9. Spatial features of scattered sampled plots within the old-growth core area at Valle Cervara. (Top) Topographic map with 25-m contour intervals and the location of sampled plots (colored circles). Black solid circle or triangle inside the plot identifies the sampling year; plot circle color refers to the shape of the diameter distribution (see Figs. 2 and 3 and for explanation of codes) when absence of a dbh class in a plot was coded as a missing value. Although there is no overlap between the location of 2003 and 2010 plots, they were both well distributed inside the core area. (Bottom) Sample (black circles) and model (red curve) semivariogram computed for the dbh distribution shapes mapped above, showing that the dominant forest structure (mostly the rotated sigmoid) tends to be maintained up to distances of about 60 m. The formula for the exponential model variogram is shown in the figure, with Co = nugget; C = sill; Ao = one-third of the effective range (57.6 m), which is the distance at which the total sill (C + Co) is within 5% of the asymptote (the sill never meets the asymptote in the exponential model); R2 = coefficient of determination; RSS = residual sum of squares. (For interpretation of the references to color in this figure legend, the reader is referred to the web version of this article.)

increasing-*q* curves, the rotated sigmoid shape was always the dominant model starting at 0.6–0.8 ha aggregated spatial scales. A few unimodal distributions were also revealed at the smallest aggregated scales (<0.3 ha), and were more common in the less structured forest (Coppo del Principe). While reporting as zero the absence of a dbh class within a plot led to an underestimation of intermediate size classes, convergence of tree distribution shapes to the rotated sigmoid was rapidly obtained regardless of coding choices. When the sampled area was progressively expanded using concentric plots, the rotated sigmoid shape became

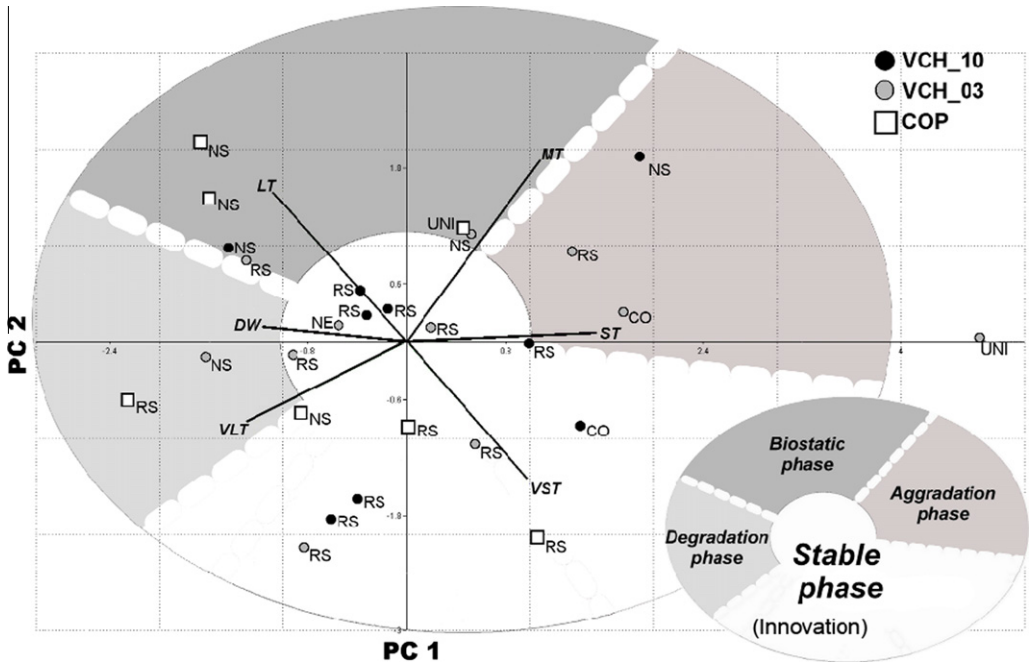

Fig. 10. Principal component analysis of tree abundance at all scattered plots (both sampling years and sites). Biplot axes were overlaid on the first two principal component axes. Diameter distribution models (with codes as explained in Figs. 2 and 3; absence of a dbh class in a plot was considered a missing value) are shown next to symbols (solid black circle = Valle Cervara 2010; solid gray circle = Valle Cervara 2003; empty square = Coppo del Principe 2010). Phases of the structural forest cycle (lower right insert) could be identified in a counterclockwise order.

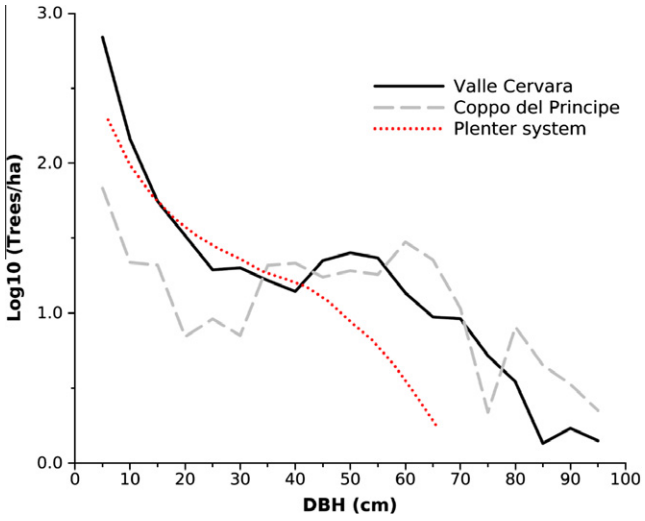

Fig. 11. Comparison between mean stand diameter distributions at Valle Cervara core area (average of 2003 and 2010 scattered plots) and Coppo del Principe vs. the *Langula* beech forest equilibrium distribution obtained using the plenter system (Schütz, 2006).

dominant even on smaller scales (0.5 ha). These small spatial scales are consistent with results obtained by Janowiak et al. (2008) despite the differences in target ecosystems and sampling methods.

The well-defined uneven-aged structure even of single plots indicated that structural forest processes controlling stand dynamics can be found in areas as small as 1200 m^2. At the same time, it became clear that an average q-value (the ratio between the density of a dbh size class and that of the next larger one, see Rubin et al., 2006) could not be computed. While the most appropriate sampling area to fully describe the forest still depends on dendrometric features (e.g. total basal area, maximum dbh), a 1-ha spatial scale was sufficient to correctly represent the dbh distribution curve in this uneven aged temperate ecosystem.

Natural stand dynamics of European temperate deciduous and mixed forests have generally been described by the "forest cycle" concept (Watt, 1947; Korpel, 1995). Our results highlight that the old-growth forest mosaic is not fully captured when structure is described only by patches in different phases of development (e.g. Remmert, 1991; Emborg et al., 2000). In fact, we propose that a fine-grain pattern, whose complex structure can be seen in a vertical transect (Fig. 1), is a common feature of old-growth beech forests when disturbance impacts are generally limited to individual trees (fine scale disturbance; Podlaski, 2008), so that resulting canopy gaps are relatively small (<200–300 m^2; Wagner et al., 2010). It is worth noting that in the dominant stratum of beech old-growth forests, tree age cannot be easily inferred from stem size (Piovesan et al., 2005b, 2010) because structural dynamics, in a very fine grain mosaic, condition individual life history. Such complex structures, also described by mixtures of theoretical size distributions, are now increasingly being reported for uneven-aged, pure or mixed, beech forests (Paluch, 2007; Podlaski, 2010). When size distribution follows the rotated sigmoid shape, these structures have been placed outside of the forest cycle and described as a "steady state" (Král et al., 2010). While our data, collected in old-growth forests that host individuals with the longest life cycle for the species, confirm the stability of this aggregated structure over several years (Fig. 8), further studies should focus on the temporal evolution of the RS shape at scales of about 0.1 ha with special regard to regeneration and disturbance processes.

Within a fine-grain forest mosaic, one development phase may locally dominate, and eventually stand structure at the single plot level changes over time following the classical forest cycle (Watt, 1947; Oldemann, 1990), as shown by the counterclockwise ordering of sampled plots in a structural cycle (Fig. 10 and Fig. S8). This synchronization of stand dynamics can also be driven by intermediate (0.04–0.5 ha) or coarse (>0.5 ha) scale disturbance events (Podlaski, 2008). Dendroecological analyses have shown that some past growth releases were synchronous between Valle Cervara (Piovesan et al., 2005b) and Coppo del Principe (Piovesan et al., 2010) testifying that in addition to small-scale gap phase

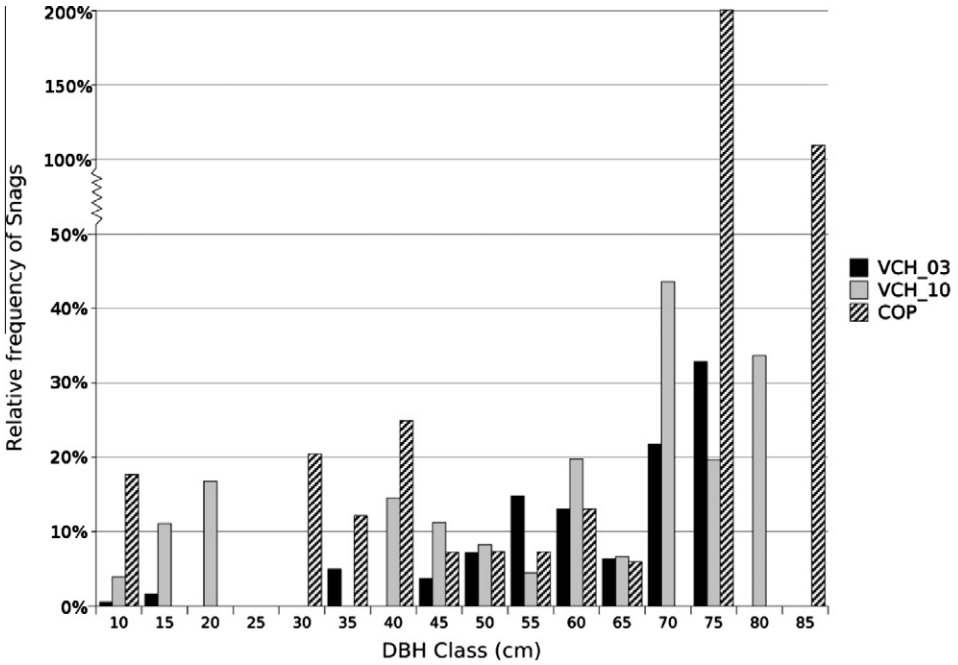

Fig. 12. Snag/living trees size distribution at Valle Cervara core area in 2003 (VCH_03) and 2010 (VCH_10), and at Coppo del Principe in 2010 (COP).

processes, periodic intermediate severity disturbance events are another driver of forest dynamics (Splechtna et al., 2005; Nagel et al., 2007; Fraver et al., 2008; Gravel et al., 2010).

Three main mechanisms are likely behind the generation of a rotated sigmoid structure (Westphal et al., 2006): infrequent disturbance at intermediate and coarse scales, as mentioned in the previous paragraph, U-shaped mortality, and nonlinear diameter increment (faster in medium-size trees compared to smaller and larger ones; see also Leak, 2002). In beech old-growth forests, snags represent about 30–40% of dead biomass (Piovesan et al., 2010; Meyer and Schmidt, 2011), but their size distribution allows an estimation of mortality rates by dbh class. Snags were not abundant, suggesting relatively low mortality, and more so at Valle Cervara than at Coppo del Principe (Fig. 12). Relative snag frequency confirmed a tendency towards higher mortality for very large trees (see also Fig. 6 in Piovesan et al., 2005b). For small sizes (up to 20 cm dbh) snags are likely an outcome of self-thinning (Coomes and Allen, 2007), while their absence in the medium size classes (25–40 cm), normally composed of trees that just reached the canopy (20–30 m height) and achieved dominance (see Fig. 4 in Piovesan et al., 2005b and table 5.2 in Peters, 1997), is closely linked to a "step-up" growth phase typical of shade-tolerant species (Leak, 2002). The 25–30 cm dbh corresponds to the inflexion point in the rotated sigmoid curve, not only in our study, but generally in old-growth beech forests (Commarmot et al., 2005). For larger sizes, snags are essentially a result of disturbance processes that leave the stem standing, such as drought. It is intriguing that snags recorded in 2010 at Valle Cervara were more numerous among the smallest size classes compared to 2003, since such increase in mortality of smaller trees over time is consistent with a drying trend in climate (Piovesan et al., 2008), as reported in other studies (Van Mantgem et al., 2009).

The third factor that drives the development of a rotated sigmoid curve is a strong positive relationship between diameter increment and stem size when small trees start exploiting resources freed by gap formation, followed by a stabilization of the increment as the same trees, larger and now part of the overstory, close the canopy gap (Westphal et al., 2006). We could not clearly test this relationship because our growth data, obtained from increment cores, did not include understory trees (dbh < 20–25 cm). A step-up relationship between diameter increment and tree size was evident in old-growth beech forests (see Table 5.5 in Peters, 1997). Stands managed using the plenter system, where the rotated sigmoid is still the best representation of the resulting tree distribution, feature a nonlinear relationship between stem size and radial increment (e.g. Schütz, 2006). In fact, it is surprising to find the rotated sigmoid under such a managed regime, since the largest individuals are constantly logged in the plenter system. When we compared data from plenter-managed stands and our old-growth forests, it was evident that the latter included a greater number of very large individuals, as shown by the deviation between the two rotated sigmoid curves for stems greater than 40–45 cm. Regeneration in the plenter system has to be sustained by removing large trees, which otherwise would impede renovation processes, as observed when a plenter-managed stand is left to its natural evolution (Schütz, 2006). The negative correlation we found between abundance of large trees and that of very small trees confirms why the plenter system requires logging of large trees: in the absence of naturally forming gaps (because no very large trees exist), regeneration needs to be maintained by removing the dominant trees. While the influence of diameter growth on size distributions of old-growth beech forests in the Italian Apennines requires further studies, it is already evident that the interlinking between mortality, fine-to-intermediate scale disturbances, individual life history, and growth patterns of beech trees is fundamental for the stability of the reversed sigmoid distribution.

The rotated sigmoid, whose final shape differs only slightly between areas <1 ha and larger aggregation levels under uniform bioclimatic conditions, is well representative of temperate old-growth deciduous forests (Janowiak et al., 2008). From our investigation, this model, which also emerges when larger sampling plots are used (5–10 ha; Westphal et al., 2006; Commarmot et al., 2005), is therefore a primary tool for analyzing and managing forest ecosystems (Keeton, 2006), especially those with old-growth features. For beech populations in the Italian Apennines, the rotated sigmoid structure was found in separate stands, and also in the same forest after about a decade, therefore it appears stable both in space and in time. Minimum areas (~10 ha; Emborg et al., 2000) that were supposed to be required for a continuous shifting mosaic steady

state under a relatively mild disturbance may therefore contain pockets where forest structure is complex and stable at scales an order of magnitude smaller (see also Paluch, 2007). This conclusion is even more intriguing if we consider that a stable forest mosaic should become established on areas whose size is directly proportional to the longevity of the species (Emborg et al., 2000), but our sampled forests host the oldest individuals yet identified for this species. Given that uneven-aged structures, and associated deadwood production, emerge even on an aggregated area of about 1 ha, one can conclude that small forest "islands" (e.g. few hectares) are a valuable tool for a "natural" way of managing beech populations (Jakoby et al., 2010), and should therefore provide an additional option when considering the best strategy for the conservation and preservation of old-growth beech stands in the Mediterranean basin.

Acknowledgements

University of Tuscia authors were partially funded by the 2007AZFFAK PRIN project: "Climate change and forests – Dendroecological and ecophysiological responses, productivity and carbon balance on the Italian network of old-growth beech forests". F. Biondi was funded by the Fulbright Senior Specialist program. We thank E. D'Andrea, M. Baliva and F. Natalini for their participation in field surveys and C. Sinibaldi for drawing Fig. 1.

Appendix A. Supplementary data

Supplementary data associated with this article can be found, in the online version, at doi:10.1016/j.foreco.2011.08.025.

References

Akaike, H., 1974. A new look at the statistical model identification. IEEE Transaction on Automatic Control AC-19 716–723.
Baker, P.J., Bunyavejchewin, S., Oliver, C.D., Ashton, P.S., 2005. Disturbance history and historical stand dynamics of a seasonal tropical forest in western Thailand. Ecological Monographs 75, 317–343.
Brown, J.H., Gillooly, J.F., Allen, A.P., Savage, V.M., West, G.B., 2004. Toward a metabolic theory of ecology. Ecology 85, 1771–1789.
Commarmot, B., Bachofen, H., Bundziak, Y., Bürgi, A., Ramp, B., Shparyk, Y., Sukhariuk, D., Viter, R., Zingg, A., 2005. Structures of virgin and managed beech forests in Uholka (Ukraine) and Sihlwald (Switzerland): a comparative study. Forest Snow and Landscape Research 79, 45–56.
Coomes, D.A., Allen, R.B., 2007. Mortality and tree-size distributions in natural mixed-age forests. Journal of Ecology 95, 27–40.
D'Amato, A.W., Orwig, D.A., Foster, D.R., 2008. The influence of successional processes and disturbance on the structure of Tsuga canadensis forests. Ecological Applications 18, 1182–1199.
Emborg, J., Christensen, M., Heilmann-Clausen, J., 2000. The structural dynamics of Suserup Skov, a near-natural temperate deciduous forest in Denmark. Forest Ecology and Management 126, 173–189.
Enquist, B.J., West, G.B., Brown, J.H., 2009. Extensions and evaluations of a general quantitative theory of forest structure and dynamics. Proceedings of National Academy of Science USA 106, 7046–7051.
Feoli, E., Lagonegro, M., 1982. Syntaxonomy of beechwoods of Apennines based on IAHOPA. Vegetatio 50, 129–173.
Fraver, S., Jonsson, B.G., Jönsson, M., Esseen, P.A., 2008. Demographics and disturbance history of a boreal old-growth Picea abies forest. Journal of Vegetation Science 19, 789–798.
Frelich, L.E., 2002. Forest Dynamics and Disturbance Regimes. Cambridge University Press, Cambridge, UK.
Goff, F.G., West, D., 1975. Canopy-understory interaction effects on forest population structure. Forest Science 21, 98–108.
Gotelli, N.J., Colwell, R.K., 2001. Quantifying biodiversity: procedures and pitfalls in the measurement and comparison of species richness. Ecology Letters 4, 379–391.
Gove, J.H., Ducey, M.J., Leak, W.B., Zhang, L., 2008. Rotated sigmoid structures in managed uneven-aged northern hardwood stands: a look at the Burr Type III distribution. Forestry 81, 161–176.
Gravel, D., Beaudet, M., Messier, C., 2010. Large-scale synchrony of gap dynamics and the distribution of understory tree species in maple–beech forests. Oecologia 162, 153–161. doi:10.1007/s00442-009-1426-6.
Grenier, Y., Blais, L., Lavoie, E., 1991. Aire minimum d'échantillonnage ou nombre se points de prisme nécessaires pour établir la structure d'un peuplement inéquienne. Canadian Journal of Forest Research 21, 1632–1638.
Gronewold, C.A., D'Amato, A.W., Palik, B.J., 2010. The influence of cutting cycle and stocking level on the structure and composition of managed old-growth northern hardwoods. Forest Ecology and Management 259, 1151–1160.
Isaaks, E.H., Srivastava, R.M., 1989. An Introduction to Applied Geostatistics. Oxford University Press, New York.
Jakoby, O., Rademacher, C., Grimm, V., 2010. Modelling dead wood islands in European beech forests: how much and how reliably would they provide dead wood? European Journal of Forest Research 129, 659–668.
Janowiak, M., Nagel, L.M., Webster, C., 2008. Spatial scale and stand structure in northern hardwood forests: implications for quantifying diameter distributions. Forest Science 54, 497–506.
Jolliffe, I.T., 1986. Principal Component Analysis. Springer-Verlag, New York.
Keeton, W.S., 2006. Managing for late-successional/old-growth characteristics in northern hardwood-conifer forests. Forest Ecology and Management 235, 129–142.
Korpel, S., 1995. Die Urwälder der Westkarpaten. G Fischer-Verlag, Stuttgart.
Král, K., Vrška, T., Hort, L., Adam, D., Šamonil, P., 2010. Developmental phases in a temperate natural spruce-fir-beech forest: determination by a supervised classification method. European Journal of Forest Research 129, 339–351.
Leak, W.B., 2002. Origin of sigmoid diameter distributions. Research Paper NE-718. Newtown Square, PA: U.S. Department of Agriculture, Forest Service, Northeastern Research Station. pp. 10.
Lines, E.R., Coomes, D.A., Purves, D.W., 2010. Influences of forest structures, climate and species composition on tree mortality across the Eastern US. PloS ONE 5(10), e13212. doi:10.1371/journal.pone.0013212.
Lorimer, C.G., Dahir, S.E., Nordheim, E.V., 2001. Tree mortality rates and longevity in mature and old-growth hemlock-hardwood forests. Journal of Ecology 89, 960–971.
Marage, D., Lemperiere, G., 2005. The management of snags: a comparison in managed and unmanaged ancient forests of the Southern French Alps. Annals of Forest Science 62, 135–142.
Meyer, P., Schmidt, M., 2011. Accumulation of dead wood in abandoned beech (*Fagus sylvatica* L.) forests in northwestern Germany. Forest Ecology and Management 261, 342–352.
Nagel, T.A., Levanic, T., Diaci, J., 2007. A dendroecological reconstruction of disturbance in an old-growth Fagus-Abies forest in Slovenia. Annals of Forest Science 64, 891–897.
Noel, J.M., Platt, W.J., Moser, E.B., 1998. Structural characteristics of old- and second-growth stands of longleaf pine (*Pinus palustris*) in the gulf coastal region of the USA. Conservation Biology 12, 533–548.
O'Hara, K.L., Gersonde, R.F., 2004. Stocking control concepts in uneven-aged silviculture. Forestry 77, 131–143.
Oldemann, R.A.A., 1990. Forests: Elements of Silvology. Springer-Verlag, Berlin, Heidelberg, New York, pp. 624.
Paluch, J.G., 2007. The spatial pattern of a natural European beech (*Fagus sylvatica* L.)–silver fir (*Abies alba* Mill.) forest: a patch-mosaic perspective. Forest Ecology and Management 253, 161–170.
Peters, R., 1997. Beech forests. Geobotany 24. Kluver Academic Publishers, The Netherlands.
Piovesan, G., Portoghesi, L., 1993. Tecniche di analisi multivariata per lo studio strutturale di un bosco di faggio. Atti del 2° Seminario "Ricerca ed esperienze nella pianificazione multifunzionale del bosco". Centro Ricerche ENEA, (23-24 November 1993), Brasimone (Bo), Italia.
Piovesan, G., Biondi, F., Bernabei, M., Di Filippo, A., Schirone, B., 2005a. Spatial and altitudinal bioclimatic zones of the Italian peninsula identified from a beech (*Fagus sylvatica* L.) tree- ring network. Acta Oecologica 27, 197–210.
Piovesan, G., Di Filippo, A., Alessandrini, A., Biondi, F., Schirone, B., 2005b. Structure, dynamics and dendroecology of an Apennine old-growth beech forest. Journal of Vegetation Science 16, 13–28.
Piovesan, G., Biondi, F., Di Filippo, A., Alessandrini, A., Maugeri, M., 2008. Drought-driven growth reduction in old beech (*Fagus sylvatica* L.) forests of the central Apennines, Italy. Global Change Biology 14, 1265–1281.
Piovesan, G., Alessandrini, A., Baliva, M., Chiti, T., D'Andrea, E., De Cinti, B., Di Filippo, A., Hermanin, L., Lauteri, M., Scarascia Mugnozza, G., Schirone, B., Ziaco, E., Matteucci, G., 2010. Structural patterns, growth processes, carbon stocks in an Italian network of old-growth beech forests. L' Italia Forestale e Montana 65, 557–590.
Piovesan, G., Alessandrini, A., Biondi, F., Di Filippo, A., Schirone, B., Ziaco, E., 2011. Bioclimatology, growth processes, longevity and structural attributes in an Italian network of old-growth beech forests spreading from the Alps to the Apennines. Beech Forests - Joint Natural Heritage of Europe. (eds. Knapp, H.D. & Fichtner, A.), BfN-Skripten 297, 173-192, Bonn-Bad Godesberg.
Podlaski, R., 2008. Dynamics in Central European near-natural *Abies-Fagus* forests: does the mosaic-cycle approach provide an appropriate model? Journal of Vegetation Science 19, 173–182.
Podlaski, R., 2010. Diversity of patch structure in Central European forests: are tree diameter distributions in near-natural multilayered Abies–Fagus stands heterogeneous? Ecological Research 25, 599–608.
R Development Core Team. (2010) R: A language and environment for statistical computing. R Foundation for Statistical Computing, Vienna, Austria. <http://www.r-project.org/>.

Remmert, H., 1991. The Mosaic-Cycle Concept of Ecosystems. Ecological Studies 85. New York, Springer. pp. 168.
Rubin, B.D., Manion, P.D., Faber-Langendoen, D., 2006. Diameter distributions and structural sustainability in forests. Forest Ecology and Management 222, 427–438.
Sagheb-Talebi, K., Schütz, J.P., 2002. The structure of natural oriental beech (*Fagus orientalis*) forests in the Caspian region of Iran and potential for the application of the group selection system. Forestry 75, 465–472.
Schütz, J.P., 2006. Modelling the demographic sustainability of pure beech plenter forests in Eastern Germany. Annals of Forest Science 63, 93–100.
Schwartz, J.W., Nagel, L.M., Webster, C.R., 2005. Effects of uneven-aged management on diameter distribution and species composition of northern hardwoods in Upper Michigan. Forest Ecology and Management 211, 356–370.
Splechtna, B.E., Gratzer, G., Black, B.A., 2005. Disturbance history of a European old-growth mixed-species forest – A spatial dendroecological analysis. Journal of Vegetation Science 16, 511–522.
Van Mantgem, P.J., Stephenson, N.L., Byrne, J.C., Daniels, L.D., Franklin, J.F., Fulé, P.Z., Harmon, M.E., Larson, A.J., Smith, J.M., Taylor, A.H., Veblen, T.T., 2009. Widespread increase of tree mortality rates in the Western United States. Science 323, 521–524.
Wagner, S., Collet, C., Madsen, P., Nakashizuka, T., Nyland, R.D., Sagheb-Talebi, K., 2010. Beech regeneration research: from ecological to silvicultural aspects. Forest Ecology and Management 259, 2172–2182.
Wang, X., Hao, Z., Zhang, J., Lian, J., Li, B., Ye, J., Yao, X., 2009. Tree size distributions in an old-growth temperate forest. Oikos 118, 25–36.
Watt, A.S., 1947. Pattern and process in the plant community. Journal of Ecology 35, 1–22.
Westphal, C., Tremer, N., von Oheimb, G., Hansen, J., von Gadow, K., Härdtle, W., 2006. Is the reverse J-shaped diameter distribution universally applicable in European virgin beech forests? Forest Ecology and Management 223, 75–83.
Zenner, E.K., 2005. Development of tree size distributions in douglas-fir forests under differing disturbance regimes. Ecological Applications 15, 701–714.